Advancing the Physics of Cosmic Distances
Proceedings IAU Symposium No. 289, 2012
Richard de Grijs, ed.

doi:10.1017/S1743921312021837

3D motions of 6.7 GHz methanol masers and effects of the Galactic bar

Naoko Matsumoto,[1] Mareki Honma,[1,2] and the *VERA* collaboration

[1]Mizusawa VLBI Observatory, National Astronomical Observatory of Japan,
2-21-1 Osawa, Mitaka, Tokyo, Japan
email: naoko.matsumoto@nao.ac.jp

[2]Department of Astronomical Science, The Graduate University for Advanced Studies (SOKENDAI), 2-21-1 Osawa, Mitaka, Tokyo, Japan
email: mareki.honma@nao.ac.jp

Abstract. To search for kinematic evidence of the existence of the Galactic bar, we observed 10 methanol maser sources at the near end of the bar with *VERA* (VLBI Exploration of Radio Astrometry). From these observations, we obtained absolute proper motions of eight sources based on the phase-referencing technique. We compared the motions with the predictions of three simple models in a 3D plane. This comparison showed that a non-flat circular rotation model and a dynamical model including a bar potential reproduce the observed data better than a flat rotation model. In addition, the bar model suggests that the inclination angle of the Galactic bar is around 35°, which is consistent with previous studies.

Keywords. masers, astrometry, Galaxy: kinematics and dynamics, radio lines: ISM

1. Introduction

VLBI observations represent a powerful approach to obtaining 3D gas kinematics. In particular, 6.7 GHz methanol-maser sources offer some advantages to trace Galactic gas based on VLBI astrometric observations (e.g., large numbers of sources, long lifetimes, and small internal proper motions), except that such observations have lower angular resolution than equivalent observations of H_2O/SiO masers, which emit at higher frequencies. Especially for Galactic bar studies, it is also advantageous that most sources are concentrated around the molecular ring in the position–velocity (PV) map (Pestalozzi *et al.* 2005).

In May 2009, 6.7 GHz receivers were newly installed at the *VERA* stations, thus introducing a capability of astrometric observations at 6.7 GHz (Matsumoto *et al.* 2011). Parallax measurements using 6.7 GHz methanol masers currently reach a distance of ∼2 kpc with *VERA*. Therefore, for distant sources near the Galactic bar, we also need to deal with proper motions in the plane of the sky at a level of mas yr^{-1}, instead of $\mathrm{km\,s^{-1}}$, because their parallaxes are too small.

2. Source selection and observations

In November 2009, we started astrometric observations of 10 methanol-maser sources with *VERA*. The exact frequency of the maser line is 6.668518 GHz ($\mathrm{CH_3OH}\,5_1 \rightarrow 6_0\,\mathrm{A}^+$). The 10 maser sources were selected from Pestalozzi *et al.* (2005) and have the following properties: (i) Galactic longitude 40° or less, (ii) declination higher than −37°, (iii) kinematic distance from the Galactic Center less than 5 kpc, (iv) flux brighter than 15 Jy (Pestalozzi *et al.* 2005) and detected with *VERA*, and (v) existence of detectable

Table 1. Observed sources and epochs for *VERA* observations.

Target source	Reference source	Separation[a]	Data epoch[b]
G 9.98−0.02	J1755−2232	3.6°	2009/339, 2010/39
G 23.01−0.41	J1825−0737	2.6°	2009/329, 2010/34, 130, 327, 2011/36, 146
G 24.78+0.08	J1825−0737	2.7°	2009/329, 2010/34, 130, 327, 2011/36, 146
G 25.65+1.04	J1825−0737	2.7°	2009/333, 2010/61, 131, 248, 2011/37, 147
G 25.70+0.04	J1834−0301	3.5°	2010/25, 99
G 28.14+0.00	J1834−0301	2.5°	2010/25, 99, 236, 317, 2011/23, 144
G 29.95−0.02	J1834−0301	3.0°	20010/26, 105, 2011/483
G 30.76−0.05	J1834−0301	3.5°	2010/26, 105, 289, 345, 2011/118
G 351.41+0.64	J1733−3722	2.7°	None[c]
G 353.40−0.36	J1733−3722	3.0°	None[c]

Notes:
[a] Separation angles between targets and reference sources.
[b] YYYY/DOY
[c] Unsuccessful in generating phase-referenced images.

Table 2. Absolute proper motions of 6.7 GHz methanol-maser sources obtained with *VERA*.

Adopted source[a]	Source name	$v_{\rm LSR}$ ($\rm km\,s^{-1}$)	$\Delta v_{\rm LSR}$[b] ($\rm km\,s^{-1}$)	$\mu_l \cos b$ ($\rm mas\,yr^{-1}$)	$\sigma_{\mu_l \cos b}$[c] ($\rm mas\,yr^{-1}$)	μ_b ($\rm mas\,yr^{-1}$)	σ_{μ_b}[c] ($\rm mas\,yr^{-1}$)
	G 9.98−0.02	42.0	(8)	−7.99	(2-point fit)	−5.76	(2-point fit)
	G 23.01−0.41	75.0	(15)	−4.33	(0.42)	−0.30	(0.18)
○	G 24.78+0.08	113.5	(9)	−6.13	(0.45)	−0.42	(0.08)
○	G 25.65+1.04	41.9	(6)	−2.10	(0.54)	−2.18	(0.05)
	G 25.70+0.04	95.3	(12)	−4.81	(2-point fit)	+3.32	(2-point fit)
○	G 28.14+0.00	101.0	(13)	−6.04	(0.25)	−0.12	(0.05)
○	G 29.95−0.02	95.5	(7)	−5.76	(0.59)	−0.11	(0.11)
○	G 30.76−0.05	91.0	(7)	−5.17	(0.79)	0.01	(0.22)
	G 351.41+0.64	−10.0	(5)	None[d]		None[d]	
	G 353.40−0.36	−20.2	(4)	None[d]		None[d]	

Notes:
[a] Sources adopted for our discussion.
[b] Velocity width.
[c] Proper-motion error.
[d] Unsuccessful in generating phase-referenced images.

phase-reference sources for use with *VERA* within 4° from the target maser sources. Our source list and data epochs are listed in Table 1.

3. Results

Fig. 1 shows the time variation of the relative positions of the maser components with respect to the phase center for each source. In our data, the synthesized beams are $\sim 3\times6$ to 5×10 mas^2.

We assumed that the observed motion is the sum of a linear proper motion and an annual parallax, and we used least-squares minimization to derive the best-fitting parameters. The fit results are shown in Fig. 1 and Table 2. Except for G 25.65+1.04, all sources exhibit a similar trend in their proper motions, i.e., the motions are much slower than the motions expected from 220 $\rm km\,s^{-1}$ Galactic rotation. In the context of our results, accurate motions for five sources were adopted for the following discussion.

https://doi.org/10.1017/S1743921312021837 Published online by Cambridge University Press

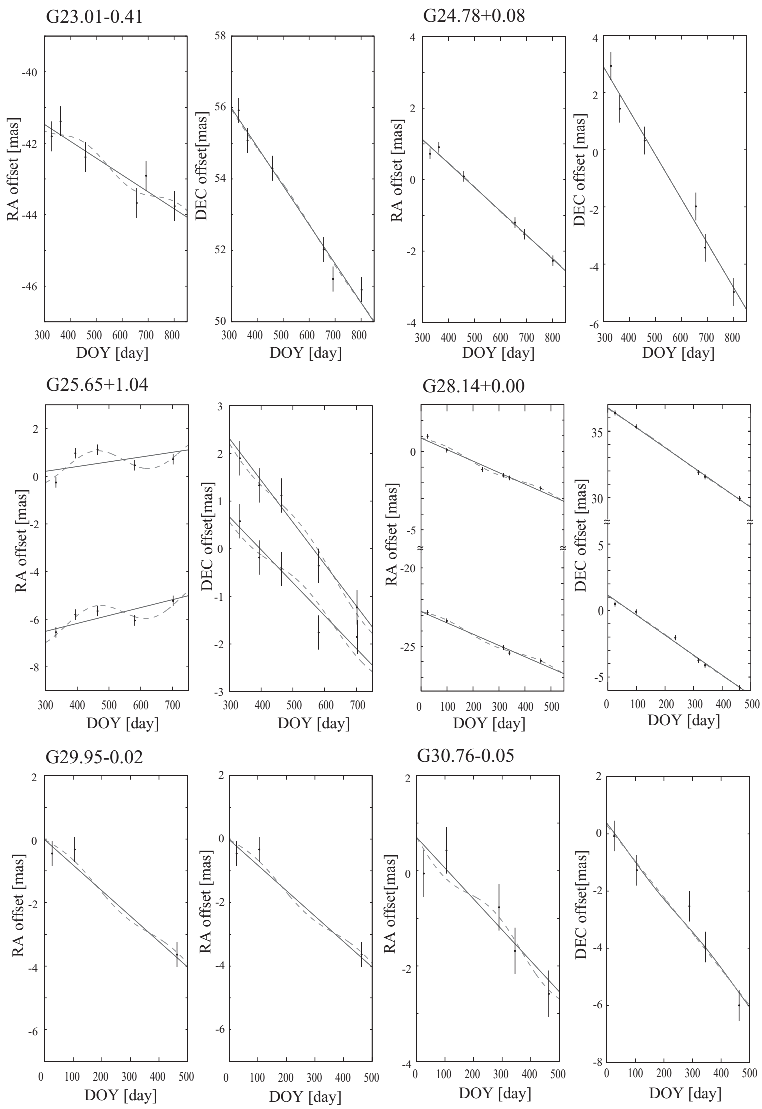

Figure 1. Results of absolute proper-motion and parallax fits. For G 23.01−0.41, G 24.78+0.08, and G 25.65+1.04, the first day is New Year's day 2009. For the other sources, the first day is New Year's day 2010. Black circles and vertical bars represent the position offsets of the maser components and the weights used for the fits, respectively. Dashed and solid lines represent the results of the least-squares fits to the absolute proper motions of the maser components, and the absolute proper motions modulated by the annual parallax, respectively.

4. Discussion

We compared the observed 3D data (Galactic longitude, in degrees, proper motions in the direction of the Galactic longitude, $\mathrm{mas\,yr^{-1}}$, and systemic velocities, in $\mathrm{km\,s^{-1}}$) with kinematic models. We additionally used data for G 23.01−0.41 and G 23.44−0.18 from Brunthaler *et al.* (2009), and for G 23.65−0.127 from Bartkiewicz *et al.* (2008), all observed with the *VLBA*. These three sources also satisfy our selection criteria.

Based on the data for the five *VERA* sources listed in Table 2 and additional data for the three *VLBA* sources, we performed least-squares fits, adopting the following three

https://doi.org/10.1017/S1743921312021837 Published online by Cambridge University Press

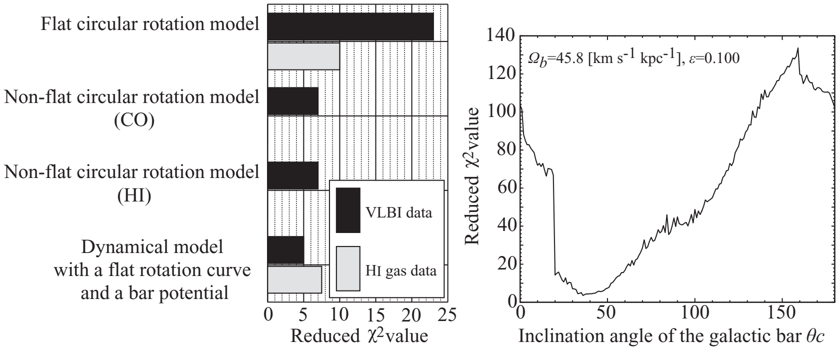

Figure 2. (left) Reduced χ^2 values of all models based on VLBI 3D data (black) and HI terminal velocities (gray). (right) Reduced χ^2 values for the inclination angle of the Galactic bar from VLBI data and a dynamical model including a bar (Wada 1994; Sakamoto *et al.* 1999).

simple models in three dimensions $(l, \mu_l \cos b, v_{\rm LSR})$. The first model is a flat rotation model with $\Theta_0 = 220$ km s^{-1}; the second model is a circular rotation model, adopting existing rotation curves based on HI/CO data (e.g., Clemens 1985; Burton & Liszt 1993; McClure-Griffiths & Dickey 2007). The final model is a dynamical model which includes the bar potential (Wada 1994; Sakamoto *et al.* 1999). We also compared the models with the terminal velocity of the HI data in the PV maps $(l, v_{\rm LSR})$. Finally, we obtained reduced χ^2 values (χ^2_ν) characterizing the match between the VLBI/HI data and each of the models (see Fig. 2, left).

We found that the VLBI data cannot be reproduced by a flat rotation model. However, our data are consistent with both existing rotation curves based on HI/CO data and the bar model. In fact, the HI data are more consistent with the model including a bar potential rather than with the flat rotation model. From a comparison of the dynamical model results and VLBI data, an acceptable inclination angle of the Galactic bar was derived at around 35° (see Fig. 2, right). This is consistent with previous studies. Thus, observed proper motions with VLBI can be explained better if we include a Galactic bar. Eventually, when more sources have been observed, we will be able to determine whether either the HI/CO rotation curves or the bar model provide a better fit, or whether other interpretations should be considered.

Acknowledgements

This work was supported by a JSPS Grant-in-Aid for Young Scientists (No. 22-171).

References

Bartkiewicz, A., Brunthaler, A., Szymczak, M., van Langevelde, H. J., & Reid, M. J. 2008, *A&A*, 490, 787
Brunthaler, A., Reid, M. J., Menten, K. M., Zheng, X. W., Moscadelli, L., & Xu, Y. 2009, *ApJ*, 693, 424
Burton, W. B. & Liszt, H. S. 1993, *A&A*, 274, 765
Clemens, D. P. 1985, *ApJ*, 295, 422
McClure-Griffiths, N. M. & Dickey, J. M. 2007, *ApJ*, 671, 427
Matsumoto, N., Honma, M., Isono, Y., *et al.* 2011, *PASJ*, 63, 1345
Pestalozzi, M. R., Minier, V., & Booth, R. S. 2005, *A&A*, 432, 737
Sakamoto, K., Okumura, S. K., Ishizuki, S., & Scoville, N. Z. 1999, *ApJ*, 124, 403
Wada, K. 1994, *PASJ*, 46, 165